

ChemComm

Accepted Manuscript



This is an *Accepted Manuscript*, which has been through the Royal Society of Chemistry peer review process and has been accepted for publication.

Accepted Manuscripts are published online shortly after acceptance, before technical editing, formatting and proof reading. Using this free service, authors can make their results available to the community, in citable form, before we publish the edited article. We will replace this *Accepted Manuscript* with the edited and formatted *Advance Article* as soon as it is available.

You can find more information about *Accepted Manuscripts* in the [Information for Authors](#).

Please note that technical editing may introduce minor changes to the text and/or graphics, which may alter content. The journal's standard [Terms & Conditions](#) and the [Ethical guidelines](#) still apply. In no event shall the Royal Society of Chemistry be held responsible for any errors or omissions in this *Accepted Manuscript* or any consequences arising from the use of any information it contains.

COMMUNICATION

Sc₃CH@C₈₀: selective ¹³C enrichment of the central carbon atom

Cite this: DOI: 10.1039/x0xx00000x

Katrin Junghans,^a Marco Rosenkranz,^a Alexey A. Popov^{*a}

Received 00th January 2012.

Accepted 00th January 2012

DOI: 10.1039/x0xx00000x

www.rsc.org/

Sc₃CH@C₈₀ is synthesized and characterized by ¹H, ¹³C, and ⁴⁵Sc NMR. A large negative chemical shift of the proton, –11.73 ppm in the *I_h* and –8.79 ppm in the *D_{5h}* C₈₀ cage isomers, is found. ¹³C satellites in the ¹H NMR spectrum enabled indirect determination of the ¹³C chemical shift for the central carbon at 174±2 ppm. Intensity of the satellites allowed determination of the ¹³C content for the central carbon atom. This unique possibility is applied to analyze the cluster/cage ¹³C distribution in mechanistic studies employing either ¹³CH₄ or ¹³C powder to enrich Sc₃CH@C₈₀ with ¹³C.

The pressure of helium gas is one of the most important parameters affecting the yield of fullerenes in the arc-discharge synthesis. Optimization of the atmosphere in the arc-discharge generator (both the pressure and composition) is even more crucial for the synthesis of endohedral metallofullerenes (EMFs) and clusterfullerenes, whose yields are usually much lower than those of empty fullerenes.¹ New types of fullerenes or their derivatives can be obtained by introducing different reagents into the arc. Stevenson et al. were the first to show that in the presence of molecular nitrogen, the nitride clusterfullerene Sc₃N@C₈₀ can be synthesized in appreciable yield.² Then, Dunsch et al. demonstrated advantages of the reactive atmosphere method in the synthesis of EMFs: The use of NH₃ as a source of nitrogen not only afforded the synthesis of nitride clusterfullerenes, but also suppressed the yield of empty fullerenes.³ The method was adopted for the synthesis of other types of EMF clusterfullerenes, such as sulfides,⁴ oxides,⁵ or certain types of carbides.^{6,7,8,9} It was also applied to stabilize unconventional empty fullerene cages via their *in situ* derivatization by hydrogen¹⁰ or chlorine atoms.¹¹ Interestingly, whereas the use of SO₂ or CO gases for the synthesis of clusterfullerenes leads to a large amount of empty fullerenes, the hydrogen-containing reagents (NH₃, CH₄, solid organic compounds¹²) suppress the yield of empty fullerenes.

Recently we have shown that methane can be advantageous for the synthesis of carbide clusterfullerenes, such as M₂TiC@C₈₀ or M₂TiC₂@C₈₀ (M is Y or a lanthanide).⁸ It is not clear if methane is barely a source of hydrogen suppressing the empty fullerene formation, or it plays a more specific role by, e.g., supplying the carbon for the endohedral cluster. Answering this question may shed more light on the fullerene formation, but the analysis of the carbon source in the EMF molecule is not straightforward. The use of isotopic substitution would be an obvious way to address this problem, but mass-spectrometry is not able to distinguish the cage and cluster atoms, whereas sensitivity of ¹³C NMR is not sufficient to allow distribution studies (detection of the central carbon atoms in carbide clusterfullerenes by ¹³C NMR required ¹³C enrichment^{9,13,14,15}). Here we circumvent this problem by studying the Sc₃CH@C₈₀, which affords ¹³C analysis of the central carbon via the ¹H NMR signal of the endohedral hydrogen and show that methane plays an active role in the formation of the endohedral cluster.

Sc₃CH@C₈₀ was synthesized in two series of experiments, using either pure Sc or a 1:1 mixture of Sc and Ti, as a source of metal. Metals were mixed with graphite powder and packed into the hole-drilled graphite rods, which were then used in the arc-discharge synthesis in the He atmosphere with an addition of several mbar of CH₄ (250 mbar total pressure). The main EMF products of the arc discharge synthesis in these conditions are Sc₄C₂@C₈₀ in pure Sc system, and Sc₂TiC@C₈₀ in the mixed-metal Sc/Ti system. Both systems afforded appreciable amounts of Sc₃CH@C₈₀, which was further isolated using HPLC (see Supporting Information for further details of separation).

Detailed characterization of Sc₃CH@C₈₀ in the first report on its synthesis was not possible due to the tiny amounts of the isolated compound.⁶ In this work, we accomplished characterization of the compound by ⁴⁵Sc, ¹³C, and ¹H NMR

spectroscopy as shown in Fig. 1. The icosahedral cage symmetry of $\text{Sc}_3\text{CH}@C_{80}$ is proved by ^{13}C NMR spectroscopy (Fig. 1a). Two cage resonances with the 3:1 intensity ratio are observed at 144.67 and 137.39 ppm, which is close to the chemical shifts reported for other clusterfullerenes with the $C_{80}-I_h$ cage¹⁶⁻¹⁹ (144.57/137.24 ppm in $\text{Sc}_3\text{N}@C_{80}$, 144.7/137.8 in $\text{Sc}_4\text{C}_2@C_{80}$,¹⁷ 144.9/137.7 ppm in $\text{Sc}_3\text{CN}@C_{80}$,¹⁸ or 144.82/137.29 ppm in $\text{Sc}_4\text{O}_2@C_{80}$ ¹⁹). In the ^{13}C -enriched sample, satellite peaks due to coupling of neighboring cage atoms can be seen (Fig. 1a) with the $^1J_{\text{CC}}$ coupling constant of 58 Hz, typical for C-sp² carbon atoms in conjugated π -systems.²⁰ Presumably, the large line-width of the endohedral carbon signal¹⁴ did not allow us to detect it in the direct ^{13}C NMR measurements, and the chemical shift of the endohedral carbon was determined from selective decoupling measurements of ^1H NMR (see below).

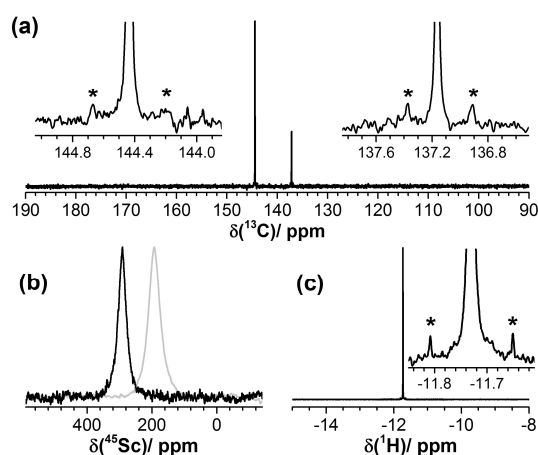


Figure 1. NMR spectra of $\text{Sc}_3\text{CH}@C_{80}$ dissolved in CS_2 : (a) 125 MHz ^{13}C NMR; (b) 121.5 MHz ^{45}Sc NMR (black line – $\text{Sc}_3\text{CH}@C_{80}$, grey line – $\text{Sc}_3\text{N}@C_{80}$); (c) 500 MHz ^1H NMR. The insets in (a) and (c) show ^{13}C satellites marked with asterisks.

In ^{45}Sc NMR spectrum, $\text{Sc}_3\text{CH}@C_{80}$ exhibits a single resonance at 292 ppm (Fig. 1b). This value is 100 ppm low-field with respect to the ^{45}Sc chemical shift in $\text{Sc}_3\text{N}@C_{80}$ at 192 ppm (Fig. 1b). The proton NMR signal of $\text{Sc}_3\text{CH}@C_{80}$ was detected at -11.73 ppm (Fig. 1c). Such a high-field value is typical for endohedral protons²¹⁻²⁴ (see Table 1). We also detected formation of the second isomer of $\text{Sc}_3\text{CH}@C_{80}$, presumably with the D_{5h} carbon cage (Fig. S6), whose ^1H NMR signal is detected at -8.79 ppm.

Table 1. ^1H and ^{13}C chemical shifts (ppm) for endohedral clusters in $\text{Sc}_3\text{CH}@C_{80}$ and selected endohedral fullerenes

EMF	$\delta(^1\text{H})$	ref	EMF	$\delta(^{13}\text{C})$	ref
$\text{Sc}_3\text{CH}@C_{80}\text{-I}^a$	-11.73		$\text{Sc}_3\text{CH}@C_{80}\text{-I}^a$	173 ± 1	
$\text{Sc}_3\text{CH}@C_{80}\text{-II}^a$	-8.79		$\text{M}_2\text{C}_2@C_{2n}^b$	220–	13,14,15,
				260	25
$\text{H}_2@C_{60}$	-1.44	21	$\text{YCN}@C_{82}$	292.4	26
$\text{H}_2\text{O}@C_{60}$	-4.81	22	$\text{Sc}_3\text{C}_2@C_{80}^-$	328.3	14
$\text{H}_2@C_{70}$	-23.97	23	$\text{Lu}_2\text{TiC}@C_{80}$	340.98	9

^a $\text{Sc}_3\text{CH}@C_{80}\text{-I}$ and $\text{Sc}_3\text{CH}@C_{80}\text{-II}$ denote the major (I_h) and the minor (presumably D_{5h}) isomers. ^b $\text{M} = \text{Sc}, \text{Y}; 2n = 80, 82, 84, 92$.

The ^1H NMR spectrum of $\text{Sc}_3\text{CH}@C_{80}$ also exhibits a low intensity doublet due to the proton-bonded ^{13}C (Fig. 1c). The $^1J_{\text{C-H}}$ coupling constant is small, 78.5 Hz, which is typical for protons bonded to carbon atoms with highly electropositive substituents. Thus, the measured $^1J_{\text{C-H}}$ constant is in line with the large negative charge on the central carbon atom predicted for $\text{Sc}_3\text{CH}@C_{80}$.²⁷ The possibility to detect ^{13}C satellites in the proton NMR spectrum enables determination of the ^{13}C chemical shift of the central carbon atom via ^1H NMR measurements with selective ^{13}C decoupling at different ^{13}C irradiation frequencies. The satellites are well visible at 165 or 180 ppm, but disappear completely at 172–175 ppm (Fig. S4). Thus, the ^{13}C chemical shift of the central atom in $\text{Sc}_3\text{CH}@C_{80}$ is determined as 173 ± 1 ppm, which is noticeably downfield than ^{13}C chemical shifts of endohedral carbons in carbide clusterfullerenes (see Table 1).

Sc_3CH and Sc_3N clusters have the same formal charge (6+) and identical electron count (the $(\text{C}^- \text{H})^{3-}$ unit is analogous to the nitride ion N^{3-}), and therefore a close similarity of the electronic properties of $\text{Sc}_3\text{CH}@C_{80}$ and $\text{Sc}_3\text{N}@C_{80}$ can be expected.^{6,27} Indeed, both compounds exhibit very similar Vis-NIR absorption spectra (Fig. 2a), with a slight blue shift of the lowest energy band in $\text{Sc}_3\text{CH}@C_{80}$ (717 nm versus 734 nm in $\text{Sc}_3\text{N}@C_{80}$). The difference is more distinct in the fluorescence spectra: whereas $\text{Sc}_3\text{CH}@C_{80}$ exhibits a NIR emission band at 835 nm, the maximum of the fluorescence band of $\text{Sc}_3\text{N}@C_{80}$ is observed at 910 nm. Crossing points of the absorption and emission bands give the optical gaps of $\text{Sc}_3\text{CH}@C_{80}$ and $\text{Sc}_3\text{N}@C_{80}$ as ca. 1.62 and 1.53 eV, respectively. The electrochemical gap of $\text{Sc}_3\text{CH}@C_{80}$ is also 0.09 V larger than that of $\text{Sc}_3\text{N}@C_{80}$ (Fig. 2b, Table 2). Both compounds exhibit similar redox behaviour with chemically irreversible first reduction near -1.2 V. DFT calculations show that $\text{Sc}_3\text{CH}@C_{80}$ and $\text{Sc}_3\text{N}@C_{80}$ have almost identical spatial distribution of the HOMO and LUMO. The HOMO is essentially a carbon cage orbital, whereas the LUMO has large contribution of Sc atoms (Fig 2c).

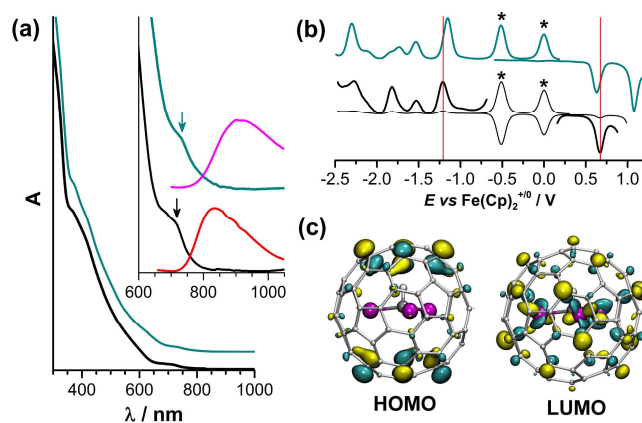


Figure 2. (a) UV-Vis spectra of $\text{Sc}_3\text{CH}@C_{80}$ (black) and $\text{Sc}_3\text{N}@C_{80}$ (cyan) in toluene, the inset shows absorption spectra in the range of the lowest energy transitions and luminescence spectra ($\text{Sc}_3\text{CH}@C_{80}$ – red, $\text{Sc}_3\text{N}@C_{80}$ – magenta; laser excitation at $\lambda_{\text{ex}} = 405$ nm); (b) Square wave voltammetry of $\text{Sc}_3\text{CH}@C_{80}$ (black) and $\text{Sc}_3\text{N}@C_{80}$ (cyan) in o-dichlorobenzene/TBAPF₄, asterisks mark $\text{Fe}(\text{Cp})_2$ and $\text{Fe}(\text{Cp}^*)_2$ used as internal standards; to guide an eye, the first reduction and oxidation potentials of $\text{Sc}_3\text{CH}@C_{80}$ are denoted with vertical red lines; (c) HOMO and LUMO of $\text{Sc}_3\text{CH}@C_{80}$ computed at the PBE/def2-TZVP level.²⁸

Table 2. Redox potentials (V) of Sc₃CH@C₈₀ and Sc₃N@C₈₀.^a

EMF	O-II	O-I	R-I	R-II	R-III	gap _{EC} ¹
Sc ₃ CH@C ₈₀		0.67	-1.21	-1.53/-1.82	-2.28	1.88
Sc ₃ CH@C ₈₀	1.09	0.63	-1.15	-1.54/-1.73		1.79

^a All potentials are determined by square-wave voltammetry in o-dichlorobenzene/TBABF₄ and are referred versus Fe(Cp)₂⁺⁰ redox couple; "O" and "R" denote oxidation and reduction, respectively

Sc₃CH@C₈₀ offers a unique possibility to study the role of methane in the carbide clusterfullerene formation using ¹³C-enrichment. The isotopic distribution of the central carbon atom can be determined by ¹H NMR from the intensity of the ¹³C satellites, whereas the net isotopic distribution in the whole molecule (dominated by that of the carbon cage) can be deduced from the mass-spectra. We synthesized ¹³C-enriched Sc₃CH@C₈₀ by applying either (i) ¹³CH₄ or (ii) ¹³C powder. To distinguish the two series, they will be denoted as "¹³CH₄/C" and "CH₄/¹³C", respectively. The amount of ¹³C powder in the CH₄/¹³C series was adjusted to keep the same amount of ¹³C in the generator as in the ¹³CH₄/C series. Figure 3 compares ¹H NMR and mass-spectra of the Sc₃CH@C₈₀ sample synthesized with the natural-abundant CH₄/C to the two types of ¹³C-enriched samples, whereas estimated ¹³C content is summarized in Table 3. In the CH₄/¹³C syntheses, the isotopic composition for the central atom and the whole molecule are both equal 5–6 % within the uncertainty limits of the NMR measurements (ca 1%). Thus, the carbon originating from the powder is equally distributed between the cage and the central atom; similar conclusion was achieved by Dorn et al. in their mass-spectrometric study of the empty fullerenes and Y-carbide clusterfullerenes.¹⁵

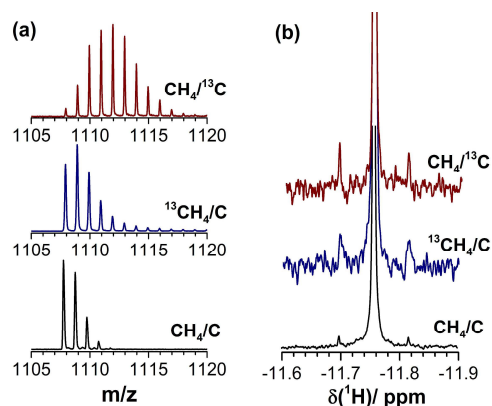


Figure 3. a) Mass-spectra of Sc₃CH@C₈₀ samples with different ¹³C content obtained in CH₄/¹³C, ¹³CH₄/C, and CH₄/C syntheses; (b) ¹H NMR spectra for the same samples, normalized to the intensity of the main singlet.

Table 3. ¹³C content for the central atom and the whole molecule

¹³ C enrichment	¹ H NMR	Mass-spectrometry
C/CH ₄ ^[a]	1.1 ± 0.4 %	1.1 ± 0.1 %
CH ₄ / ¹³ C	5.8 ± 0.9 %	5.0 ± 0.2 %
¹³ CH ₄ /C	7.6 ± 1.5 %	1.6 ± 0.1 %

^a natural abundance

Substantially different results are obtained in the ¹³CH₄/C syntheses: the ¹³C enrichment of the carbon cage is only 1.6±0.1

%, whereas the ¹³C content for the central atoms is much higher, 7.6±1.5 %. Thus, despite the rather large error bars in the NMR measurement (caused by the limited sample amount), selective ¹³C enrichment of the central carbon atom by ¹³CH₄ is beyond any doubt. The ¹³CH₄/C syntheses thus provide rich information on the Sc₃CH@C₈₀ formation process.

The volume inside the generator can be schematically divided into three zones:

- 1) The "hot" zone near the center of the arc, where the temperature is up to several thousand K,²⁹ and majority of chemical bonds (including C–H) are broken. Only the most stable species (such as C₂ dimers) can survive.
- 2) The periphery of the hot zone, where the carbon vapor cools down by the adiabatic expansion and interaction with helium atoms, resulting in a self-assembly of fullerenes and other carbonaceous structures. This intermediate zone is hot enough to provide sufficient energy for the rearrangement of the building carbon networks, but the temperature is not high enough for their atomization.
- 3) The "cold" zone, where the fullerenes can only anneal (e.g., structural defects can be healed), but substantial structural rearrangements are already not possible.

We propose that all CH₄ molecules entering the hot zone are completely atomized, and therefore the carbon atoms from methane can serve as a source of carbon for the fullerene cage. Since the hot zone occupies only a small volume, whereas methane is distributed over the whole generator chamber, only a small fraction of methane present in the system passes through the hot zone. Thus, it is not surprising that the content of methane-originating carbon atoms in the fullerene cage is not exceeding 0.5 %, whereas the main sources of carbon for both the fullerene cage and the endohedral cluster are the graphite rods and graphite powder packed into the rods.

When the C/H vapor leaves the hot zone, the CH bonds can be formed again. Note that from the 0.5% contribution of the methane as a source of carbon for the cage, the C:H ratio in the hot zone is tentatively estimated as 50:1. This ratio is sufficient for a dramatic suppression of the empty fullerene formation. The ¹³C/¹²C distribution in the newly formed CH bonds can be considered roughly equal the ¹³C content in the carbon cage (1.6 % in the ¹³CH₄/C syntheses). The fact that the ¹³C content for the central carbon atom in Sc₃CH@C₈₀ obtained in the ¹³CH₄ syntheses is several times higher than for the fullerene cage means that methane is also chemically active in the "intermediate" zone. Although CH₄ molecules are not completely atomized here, they can exchange protons with other carbon structures or react with Sc atoms to substitute protons. However, some ¹³CH fragments remain intact (else the isotopic distribution for the cage and the cluster would be equalized) and take part in the endohedral fullerene formation. The fraction of such "native" ¹³CH units in Sc₃CH@C₈₀ is the difference between the ¹³C content in the cluster and in the cage, and can be roughly estimated as 6%.

Conclusions

In this work we reported on the synthesis and spectroscopic characterization of Sc₃CH@C₈₀. Its ¹³C, ⁴⁵Sc, and ¹H NMR spectra are reported for the first time and fully establish the molecular structure of this clusterfullerene. Electronic properties of Sc₃CH@C₈₀ are similar to those of its close analog, nitride clusterfullerene Sc₃N@C₈₀. Yet, absorption and fluorescence spectroscopy as well as electrochemical study show that the bandgap of Sc₃CH@C₈₀ is higher by 0.09 eV. Most importantly, a unique possibility to determine ¹³C composition of the central atom in the cluster by via ¹H NMR enables an analysis of the role of methane in the clusterfullerene formation. A series of ¹³C enrichment with either ¹³CH₄ or ¹³C powder showed that the use of ¹³CH₄ in the synthesis of Sc₃CH@C₈₀ allows selective enrichment of the central carbon atom with ¹³C.

Acknowledgements

The authors acknowledge funding by DFG (grant PO 1602/1-2) and the European Research Council (ERC) under the European Union's Horizon 2020 research and innovation programme (grant agreement No 648295 "GraM3"). Authors thank Ulrike Nitzsche for technical assistance with computational resources in IFW Dresden.

Notes and references

^a Leibniz Institute for Solid State and Materials Research, 01069 Dresden, Germany. E-mail: a.popov@ifw-dresden.de

† Electronic Supplementary Information (ESI) available: additional experimental details, HPLC separation, FTIR and NMR spectra. See DOI: 10.1039/c000000x/

1. A. A. Popov, S. Yang and L. Dunsch, *Chem. Rev.*, 2013, **113**, 5989; X. Lu, L. Feng, T. Akasaka and S. Nagase, *Chem. Soc. Rev.*, 2012, **41**, 7723; A. Rodriguez-Fortea, A. L. Balch and J. M. Poblet, *Chem. Soc. Rev.*, 2011, **40**, 3551.
2. S. Stevenson, G. Rice, T. Glass, K. Harich, F. Cromer, M. R. Jordan, J. Craft, E. Hadju, R. Bible, M. M. Olmstead, K. Maitra, A. J. Fisher, A. L. Balch and H. C. Dorn, *Nature*, 1999, **401**, 55.
3. L. Dunsch, M. Krause, J. Noack and P. Georgi, *J. Phys. Chem. Solids*, 2004, **65**, 309; L. Dunsch, P. Georgi, M. Krause and C. R. Wang, *Synth. Met.*, 2003, **135**, 761.
4. N. Chen, M. N. Chaur, C. Moore, J. R. Pinzon, R. Valencia, A. Rodriguez-Fortea, J. M. Poblet and L. Echegoyen, *Chem. Commun.*, 2010, **46**, 4818; N. Chen, M. Mulet-Gas, Y.-Y. Li, R. E. Stene, C. W. Atherton, A. Rodriguez-Fortea, J. M. Poblet and L. Echegoyen, *Chem. Sci.*, 2013, **4**, 180; N. Chen, C. M. Beavers, M. Mulet-Gas, A. Rodriguez-Fortea, E. J. Munoz, Y.-Y. Li, M. M. Olmstead, A. L. Balch, J. M. Poblet and L. Echegoyen, *J. Am. Chem. Soc.*, 2012, **134**, 7851; F.-F. Li, N. Chen, M. Mulet-Gas, V. Triana, J. Murillo, A. Rodriguez-Fortea, J. M. Poblet and L. Echegoyen, *Chem. Sci.*, 2013, **4**, 3404.
5. T. Yang, Y. Hao, L. Abella, Q. Tang, X. Li, Y. Wan, A. Rodriguez-Fortea, J. M. Poblet, L. Feng and N. Chen, *Chem.-Eur. J.*, 2015, **21**, 11110; M. Zhang, Y. Hao, X. Li, L. Feng, T. Yang, Y. Wan, N. Chen, Z. Slanina, F. Uhlik and H. Cong, *J. Phys. Chem. C*, 2014, **118**, 28883; Q. Tang, L. Abella, Y. Hao, X. Li, Y. Wan, A. Rodriguez-Fortea, J. M. Poblet, L. Feng and N. Chen, *Inorg. Chem.*, 2015, **54**, 9845.
6. M. Krause, F. Ziegls, A. A. Popov and L. Dunsch, *ChemPhysChem*, 2007, **8**, 537.
7. A. L. Svitova, K. Ghiassi, C. Schlesier, K. Junghans, Y. Zhang, M. Olmstead, A. Balch, L. Dunsch and A. A. Popov, *Nat. Commun.*, 2014, **5**, 3568; Y. Feng, T. Wang, J. Wu, Z. Zhang, L. Jiang, H. Han and C. Wang, *Chem. Commun.*, 2014, **50**, 12166.
8. Q. Deng, K. Junghans and A. A. Popov, *Theor. Chem. Acc.*, 2015, **134**, 10.
9. K. Junghans, C. Schlesier, A. Kostanyan, N. A. Samoylova, Q. Deng, M. Rosenkranz, S. Schiemenz, R. Westerström, T. Greber, B. Büchner and A. A. Popov, *Angew. Chem.-Int. Edit. Engl.*, 2015, **54**, 13411.
10. C. R. Wang, Z. Q. Shi, L. J. Wan, X. Lu, L. Dunsch, C. Y. Shu, Y. L. Tang and H. Shinohara, *J. Am. Chem. Soc.*, 2006, **128**, 6605.
11. Y.-Z. Tan, X. Han, X. Wu, Y.-Y. Meng, F. Zhu, Z.-Z. Qian, Z.-J. Liao, M.-H. Chen, X. Lu, S.-Y. Xie, R.-B. Huang and L.-S. Zheng, *J. Am. Chem. Soc.*, 2008, **130**, 15240; Y. Z. Tan, J. Li, F. Zhu, X. Han, W. S. Jiang, R. B. Huang, Z. P. Zheng, Z. Z. Qian, R. T. Chen, Z. J. Liao, S. Y. Xie, X. Lu and L. S. Zheng, *Nat. Chem.*, 2010, **2**, 269; S. Y. Xie, F. Gao, X. Lu, R. B. Huang, C. R. Wang, X. Zhang, M. L. Liu, S. L. Deng and L. S. Zheng, *Science*, 2004, **304**, 699; Y.-Z. Tan, R.-T. Chen, Z.-J. Liao, J. Li, F. Zhu, X. Lu, S.-Y. Xie, J. Li, R.-B. Huang and L.-S. Zheng, *Nat. Commun.*, 2011, **2**, 420; Y.-Z. Tan, S.-Y. Xie, R.-B. Huang and L.-S. Zheng, *Nat. Chem.*, 2009, **1**, 450.
12. S. Yang, L. Zhang, W. Zhang and L. Dunsch, *Chem.-Eur. J.*, 2010, **16**, 12398; M. Jiao, W. Zhang, Y. Xu, T. Wei, C. Chen, F. Liu and S. Yang, *Chem.-Eur. J.*, 2012, **18**, 2666; F. Liu, J. Guan, T. Wei, S. Wang, M. Jiao and S. Yang, *Inorg. Chem.*, 2013, **52**, 3814.
13. X. Lu, T. Akasaka and S. Nagase, *Acc. Chem. Res.*, 2013, **46**, 1627; H. Kurihara, X. Lu, Y. Iiduka, N. Mizorogi, Z. Slanina, T. Tsuchiya, T. Akasaka and S. Nagase, *J. Am. Chem. Soc.*, 2011, **133**, 2382; J. Zhang, T. Fuhrer, W. Fu, J. Ge, D. W. Bearden, J. L. Dallas, J. C. Duchamp, K. L. Walker, H. Champion, H. F. Azurmendi, K. Harich and H. C. Dorn, *J. Am. Chem. Soc.*, 2012, **134**, 8487.
14. Y. Yamazaki, K. Nakajima, T. Wakahara, T. Tsuchiya, M. O. Ishitsuka, Y. Maeda, T. Akasaka, M. Waelchli, N. Mizorogi and H. Nagase, *Angew. Chem.-Int. Edit. Engl.*, 2008, **47**, 7905.
15. J. Zhang, F. L. Bowles, D. W. Bearden, W. K. Ray, T. Fuhrer, Y. Ye, C. Dixon, K. Harich, R. F. Helm, M. M. Olmstead, A. L. Balch and H. C. Dorn, *Nat. Chem.*, 2013, **5**, 880.
16. T. Wang and C. Wang, *Acc. Chem. Res.*, 2014, **47**, 450.
17. T.-S. Wang, N. Chen, J.-F. Xiang, B. Li, J.-Y. Wu, W. Xu, L. Jiang, K. Tan, C.-Y. Shu, X. Lu and C.-R. Wang, *J. Am. Chem. Soc.*, 2009, **131**, 16646.
18. T.-S. Wang, L. Feng, J.-Y. Wu, W. Xu, J.-F. Xiang, K. Tan, Y.-H. Ma, J.-P. Zheng, L. Jiang, X. Lu, C.-Y. Shu and C.-R. Wang, *J. Am. Chem. Soc.*, 2010, **132**, 16362.
19. A. A. Popov, N. Chen, J. R. Pinzón, S. Stevenson, L. A. Echegoyen and L. Dunsch, *J. Am. Chem. Soc.*, 2012, **134**, 19607.
20. K. Kamińska-Trela, in *Annual Reports on NMR Spectroscopy*, ed. G. A. Webb, Academic Press, 1995, pp. 131.
21. K. Komatsu, M. Murata and Y. Murata, *Science*, 2005, **307**, 238.
22. K. Kurotobi and Y. Murata, *Science*, 2011, **333**, 613.
23. M. Murata, S. Maeda, Y. Morinaka, Y. Murata and K. Komatsu, *J. Am. Chem. Soc.*, 2008, **130**, 15800.
24. A. Krachmalnicoff, R. Bounds, S. Mamone, M. H. Levitt, M. Carravetta and R. J. Whitby, *Chem. Commun.*, 2015, **51**, 4993; E. E. Marotto, J. Mateos, M. Garcia-Borràs, S. Osuna, S. Filippone, M. Á. Herranz, Y. Murata, M. Solà and N. Martín, *J. Am. Chem. Soc.*, 2015, **137**, 1190.
25. X. Lu, K. Nakajima, Y. Iiduka, H. Nikawa, N. Mizorogi, Z. Slanina, T. Tsuchiya, S. Nagase and T. Akasaka, *J. Am. Chem. Soc.*, 2011, **133**, 19553.
26. S. Yang, C. Chen, F. Liu, Y. Xie, F. Li, M. Jiao, M. Suzuki, T. Wei, S. Wang, Z. Chen, X. Lu and T. Akasaka, *Sci. Rep.*, 2013, **3**, 1487.
27. A. A. Popov and L. Dunsch, *Chem.-Eur. J.*, 2009, **15**, 9707.
28. J. P. Perdew, K. Burke and M. Ernzerhof, *Phys. Rev. Lett.*, 1996, **77**, 3865; F. Neese, *WIREs Comput. Mol. Sci.*, 2012, **2**, 73; W. Humphrey, A. Dalke and K. Schulten, *J. Molec. Graphics*, 1996, **14**, 33.
29. H. Lange, K. Saidane, M. Razafinimanana and A. Gleizes, *Journal of Physics D: Applied Physics*, 1999, **32**, 1024.